MODE-I FRACTURE TOUGHNESS OF INTERLAYERED EPOXY ADHESIVES

Dharun, Vadugappatty Srinivasan[a], Anastasios P.Vassilopoulous[a]

a: Composite Construction Laboratory (CCLab), Ecole Polytechnique Fédérale de Lausanne
EPFL, Station 16, CH-1015 Lausanne, Switzerland.
dharun.srinivasan@epfl.ch

Abstract: *Epoxy adhesives are commonly used in the assembly of primary engineering structures such as aircraft, wind turbines, yachts and bridges. Damages in the adhesive bond line can lead to sudden fracture. Crack arresting features (CAFs) like rivets, bolts and other mechanical fasteners are used in these structures at the penalty of additional assembly cost and weight. This paper endeavors to the crack arresting effect of polyvinylidene fluoride (PVDF) and polyetherimide (PEI) thermoplastic layers under mode-I plane strain fracture. Non-toughened and toughened epoxy adhesives are used to fabricate the reference samples. The constitutive properties of the adhesives, PVDF and PEI are measured through uniaxial tensile testing. PVDF and PEI layers of 0.5 mm thickness are incorporated in the adhesives and mode-I fracture toughness is determined through single-edge-notched bending (SENB). Experimental test results show that these layers can arrest the cracks effectively at the layer interface***.**

Keywords: Adhesives; fracture toughness; thermoplastic layer; crack shielding.

1. Introduction

Adhesive bonding is used in primary engineering structures however its full potential could not be realized due to its low reliability. Cracks emerging from the inherent defects, in-service damages and high stress concentrated regions are arrested by mechanical fasteners such as bolts and rivets. Disbond, weak bond and impact damage induced disbond are the sources of failure initiation in the adhesive joints. The three main requirements of crack arresting features are (i) stopping the disbond at a pre-determined allowable length (b) meeting the desired design loading requirements (c) load-bearing capability that can be determined by reliable and repeatable non-destructive inspection (NDI) methods. One of the three criteria should be met to get certified by the air transportation authorities [1]. In composite materials, delaminations were arrested by through thickness reinforcement such as Z pins. T. Lobel et al. [2] used staple pins with dry fabrics before resin transfer molding and the measured double lap shear strength was 28 % higher than the conventional rivets. Thanks to the axial fixation and no pull out of the staple pins. Nevertheless, Z pins and staple pins were limited to co-bonding and co-curing. The challenge remains in secondary bonding applications. T. Kruse et al. [3] showed that the cracked lap shear sample designed with lock bolts of 4 mm to 4.8 mm diameter could offer better fatigue crack growth resistance as compared with the reference sample. The crack growth was also slowed down by the laser ablation technique in which the carbon fibers of the adherend bond surface were exposed before bonding [4]. Fastener-adhesive hybrid bonding provides a crack arresting mechanism in three ways (a) closing crack tip by fastener axial stiffness (b) crack friction by fastener preloading and (c) fastener-joint shear stiffness [5]. Selective toughening can be applied to areas that require local toughening, such as free edges, holes and highly stressed regions. Local toughening reduces the manufacturing cost or decreases the adverse effect of

total toughening. In a single-ply interface toughening, unstable crack growth was observed as the crack was propagated from a high fracture toughness to a lower fracture toughness material [6]. A ductile phase thermoplastic was incorporated to arrest the disbond, a fail-safe design methodology to ease the certification requirements. Although the initial crack was unstable and the strain energy release rate was even smaller than the reference value, the crack was stopped as it reached the thermoplastic [1]. The crack was unstable as it penetrated through the PVDF layer. Crack tip blunting is another toughening strategy that was realised by stop holes in the adhesive joint. Fracture toughness can also be increased up to 120% by incorporating copper (Cu) wire mesh in the adhesive bond line[7].

Several studies reveal that extrinsic toughening through interlayers is a promising technique but there are no clear material design guidelines to aid practical applications and their fracture behaviour should be explored. In this study, two thermoplastic layers with 0.5 mm thickness are interlayered with non-toughened and toughened adhesives and their crack arresting effect was investigated through mode-I plane-strain fracture toughness testing. Additionally, the constituent properties of the adhesives, PVDF and PEI materials are determined through tensile testing.

2. Materials and manufacturing

SPABOND™ (SP) 820HTA and SPABOND™ 840HTA are epoxy paste adhesives, provided by Gurit (UK) Ltd. SP 820HTA is a non-toughened adhesive and primarily modified with glass fibers (BB) whereas SP 840HTA is toughened with core-shell rubber particles (TT). Kynar® PVDF and Ultem® 1000 PEI are high-performance structural thermoplastic interlayers, procured from Emco Industrial Plastics, Inc, USA.

The epoxy base and hardener were mixed at a ratio of 100:33 using a wooden spatula and degassed at 0.95 bar of vacuum for 5 to 10 minutes and filled into a mold cavity. Initially, the adhesive was cured at room temperature (24°C ± 2°C) for 120 minutes and oven-cured for 120 minutes at 70°C. The heating and cooling rate was set to 2°C/min and 5 °C/min. For interlayering, PVDF and PEI layers were sanded with a 60-grit size paper using Bosch sanding tool. The dirt particles were removed by tap water and the layers were conditioned at 40°C for 10 minutes. Meanwhile, 5 g of mixed adhesive was diluted with 25 g of isopropanol as a primer. The primer solution was coated over the layers and dried at room temperature for 30 minutes. The mold cavity was partially filled (15 mm + $\Delta a_{pre\ CAF}$) and the primer coated layer having a thickness of 0.5 mm (t) was placed before filling the remaining adhesive. $\Delta a_{pre\ CAF}$, a distance between the thermoplastic layer and the initial crack length (see Figure 1) was arbitrarily selected as 6.75 mm to understand the dynamic crack arresting behaviour. Table 1 shows the various material configurations used for fracture toughness testing.

Table 1. Material design details of pristine and interlayered epoxy adhesives.

S.no	Sample	Adhesive	Interlayer Material	Interlayer Thickness (t) (mm)	Position ($\Delta a_{pre\ CAF}$) (mm)
1	BB	BB	-	-	-
2	TT	TT	-	-	-
3	BBPVDF	BB	PVDF	0.5	6.75
4	BBPEI	BB	PEI	0.5	6.75

Abrasive water-jet machining was used for cutting the thermoplastic layers to the required nominal dimensions for the tensile and SENB testing. The geometrical dimensions S, W and B are 120 mm, 30 mm and 15 mm, respectively (see Figure 1). In the SENB samples, an initial notch was machined by a rotary saw and further sharpened with an abrasive paste and a razor blade. The initial crack length (a) of prepared samples was measured through an optical microscope, Dino-Lite AD7013MZT. To use the digital image correlation (DIC) technique, all the tensile and SENB samples were uniformly coated at least twice with white paint, dried and then sprinkled with the black speckles.

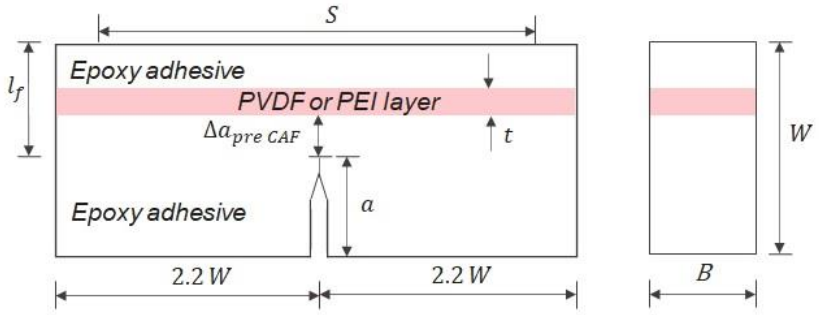

Figure 1. Schematic diagram of thermoplastic interlayered SENB test sample.

3. Tensile and SENB testing

Uniaxial tensile test was conducted using MTS® 810 Landmark servo-hydraulic machine with a calibrated load cell capacity of 5 kN and applied force accuracy of ±5%. ASTM D638-14 Type II samples of adhesives and Type I samples of PVDF and PEI were tested under displacement control, at a crosshead rate of 1 mm/min. All the tests were performed at the ambient temperature of 22 ± 3°C and relative humidity of 40 ± 10%.

Walter + bai (w + b) test machine equipped with a load cell capacity of 50 kN and a three-point bending fixture was used for the plane strain fracture toughness testing. The sample was adjusted in the fixture such that the initial notch and the contact point of the top roller were on the same loading axis. The top roller was loaded at a displacement rate of 0.25 mm/min to have a stable fracture. During the testing, 2D DIC images were captured from which the mid-span deflection was calculated. To have an effective K_{IC}, the load P_Q was selected as mentioned in ASTM D5045-14.

4. Results and discussion

The true tensile stress versus strain response of the pristine adhesives and interlayered adhesives are shown in Figure 2a. All the samples showed initial linear-elastic behaviour and followed by a non-linear response. Among the tested materials, PVDF showed a very high strain to failure whereas PEI exhibited high tensile strength. The tensile modulus of BB adhesive is higher than the other materials. Longitudinal strain versus lateral strain response of the materials is shown in Figure 2b from which the elastic and plastic Poisson's ratio were calculated. Poisson's ratio of BB adhesive was constant until the final failure. In TT and PVDF, the Poisson's ratio was decreased in the plastic region. Due to PEI softening, there was a slight increase in the Poisson's ratio after the linear elastic region.

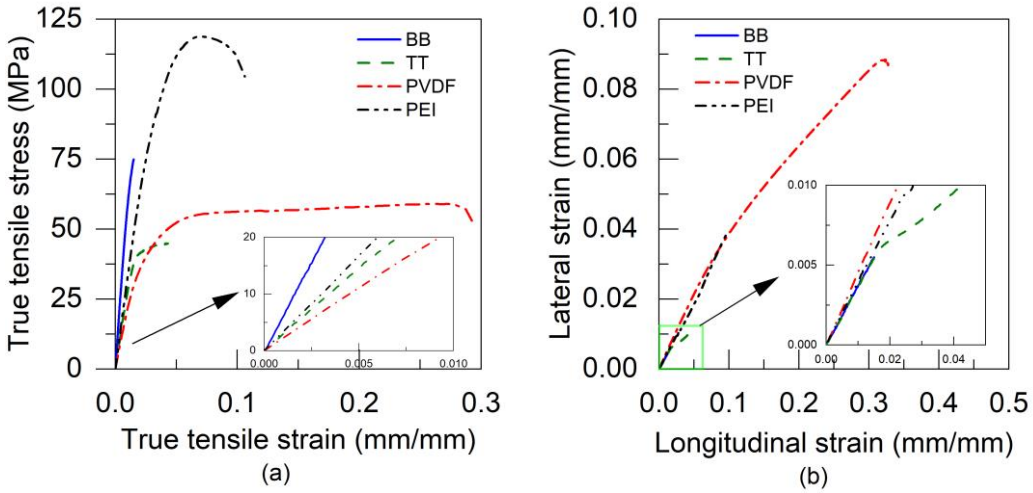

Figure 2. Tensile properties of adhesives, PVDF and PEI: (a) true stress versus strain and (b) longitudinal to lateral strain response.

The tensile properties of the adhesives, PVDF and PEI are shown in Table 2. The tensile modulus of TT and PVDF are comparable. In this case, the yield strength is different which can be referred to as yield strength inhomogeneity.

Table 2. Tensile properties of the epoxy adhesives, PVDF and PEI.

Properties	BB	TT	PVDF	PEI
Tensile modulus (E), GPa	5.59±0.39	2.81±0.16	2.21±0.11	3.44±0.10
0.2% offset Yield stress (σ_y), MPa	61.47±1.75	37.86±0.55	31.09±1.02	67.45±2.99
Tensile strength (σ_u), MPa	69.01±0.51	44.47±1.26	58.03±0.78	117.43±2.13
Failure strain (ε_f), mm/mm	0.0170±0.001	0.0417±0.005	0.238±0.035	0.064±0.008
Tensile toughness (U_T), kJ/m^3	0.71±0.03	1.45±0.20	13.78±1.95	7.35±2.52
Elastic Poisson's ratio	0.374±0.004	0.36±0.002	0.457±0.008	0.337±0.02
Plastic Poisson's ratio	-	0.18±0.018	0.243±0.026	0.43±0.01

Tensile failure images of PVDF and PEI samples are shown in Figure 3a and 3b, respectively. Whitening due to severe plastic deformation was observed in PVDF whereas the necking phenomenon was noticed in PEI.

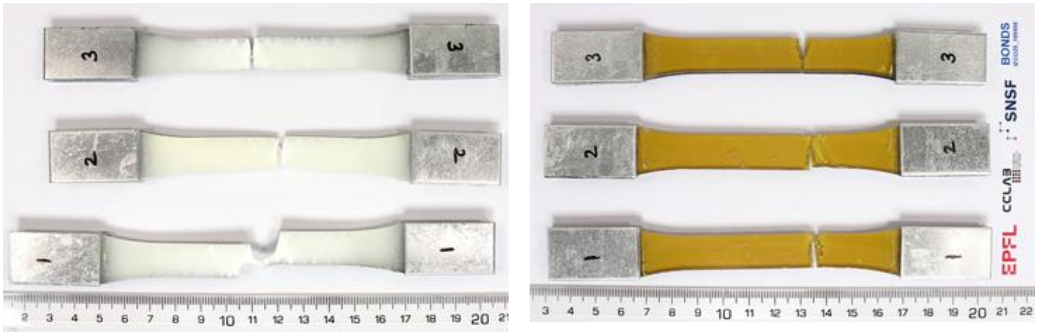

Figure 3. Tensile failure of the thermoplastics: (a) PVDF and (b) PEI.

The force versus deflection response of the pristine and interlayered SENB samples are compared in Figure 4. After reaching the initial peak load, a very small crack resistance was offered by BB adhesive whereas TT adhesive failed abruptly, exhibiting unstable crack propagation. K_{IC} of BB and TT adhesive were calculated as 2.95±0.19 $Mpa\sqrt{m}$ and 2.17±0.01 $Mpa\sqrt{m}$. In BBPVDF, the crack was stopped by the PVDF layer at a load of 277.05±19.60 N and then it started to grow along with the interface. After reaching the second peak load of 802.53±26.59 N, the crack propagated through the PVDF resulting in unstable fracture. Similarly, the crack was arrested at 237.58±9.03 in BBPEI sample and grown at the interface before failing at 734.25±10.08 N. The K_{IC} of BBPVDF and BBPEI are 2.77±0.05 and 2.70±0.05 respectively. The crack arresting load and failure load of PVDF interlayered epoxies are higher than PEI interlayering. However, PEI interlayered epoxies absorbed more fracture energy (3244±63.5 Nmm, area under the curve) than all samples.

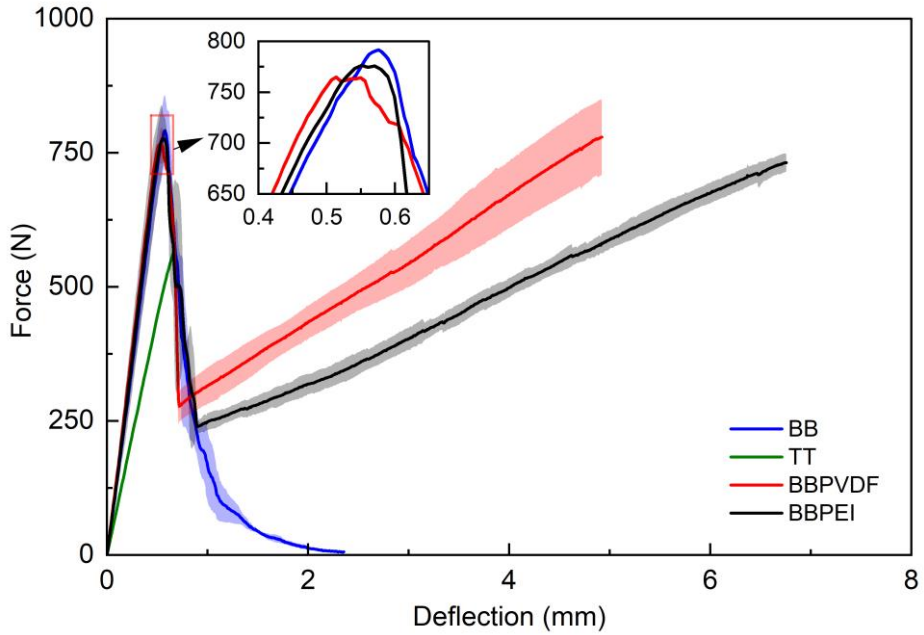

Figure 4. Force versus deflection response of pristine and thermoplastic interlayered adhesives.

Figure 5a and 5b show the crack initiation and propagation at BB sample, respectively. The crack path was slightly deviated from the initial crack plane which can explain the increase in K_{IC} value as compared to the technical data sheet value. Figure 5a reveals the interaction between the crack and PEI interlayer in BBPEI sample. After the arrest load, the force was increased to another peak as the interface crack was started growing.

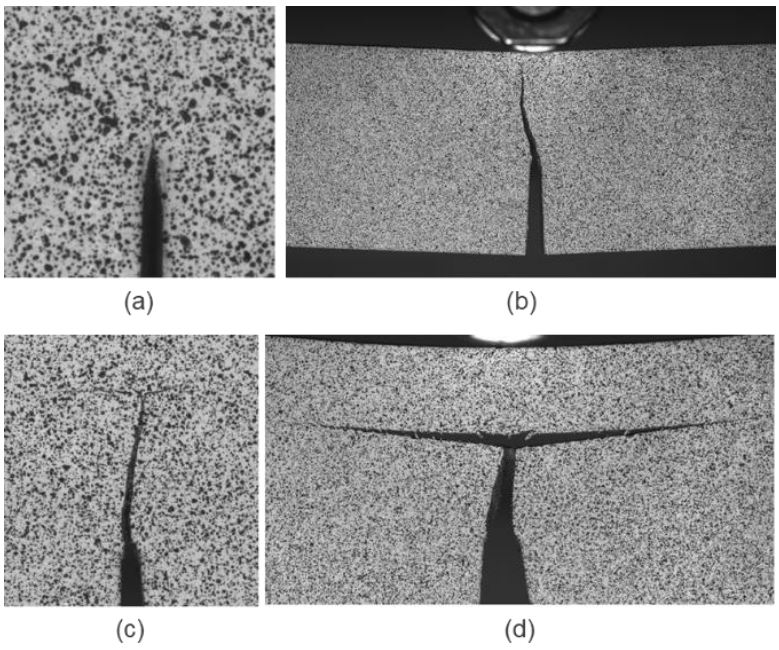

Figure 5. Failure behaviour of the samples: (a) crack initiation at BB, (b) final failure of BB, (C) crack interacting at PEI layer of BBPEI and (d) interface crack growing before the final failure at BBPEI.

5. Conclusion

The constitutive properties of the adhesives and thermoplastic layers were determined by the uniaxial tensile test. Further incorporating the PVDF or PEI thermoplastic layer, the mode-I crack could be stopped at the layer interface. As compared to PEI, PVDF layer showed a higher crack arresting and final failure load. In the future, the effect of thermoplastic layer position with respect to initial crack and layer thickness will be investigated.

Acknowledgements

The authors wish to acknowledge the support and funding of this research by the Swiss National Science Foundation (Grant No. IZCOZ0_189905) under the project, Bonded composite primary structures in engineering applications (BONDS). The authors also acknowledge the experimental assistance provided by the technical team of the structural engineering experimental platform (GIC-ENAC) at the Ecole Polytechnique Fédérale de Lausanne (EPFL), Switzerland. The authors also thank Gurit UK Ltd for providing adhesive materials. This article/publication is based upon work from COST Action CA18120 (CERTBOND - https://certbond.eu/), supported by COST (European Cooperation in Science and Technology).

6. References

1. Löbel T, Holzhüter D, Sinapius M, Hühne C. A hybrid bondline concept for bonded composite joints. International Journal of Adhesion and Adhesives. 2016; 68:229–38.
2. Löbel T, Kolesnikov B, Scheffler S, Stahl A, Hühne C. Enhanced tensile strength of composite joints by using staple-like pins: Working principles and experimental validation. Composite Structures. 2013; 106:453–60.
3. Kruse T, Körwien T, Ruzek R. Fatigue behaviour and damage tolerant design of composite bonded joints for aerospace application. ECCM 2016 - Proceeding of the 17th European Conference on Composite Materials. 2016; 7–9.
4. Kruse T, Körwien T, Heckner S, Geistbeck M. Bonding of CFRP primary aerospace structures - Crackstopping in composite bonded joints under fatigue. ICCM International Conferences on Composite Materials. 2015; 19–24.
5. Richard L, Lin KY. Delamination / Disbond Arrest Features in Aircraft Composite Structures. 2014; 3–6.
6. Malkin R, Trask RS, Bond IP. Control of unstable crack propagation through bio-inspired interface modification. Composites Part A: Applied Science and Manufacturing. 2013; 46(1):122–30.
7. Maloney K, Fleck N. Toughening strategies in adhesive joints. International Journal of Solids and Structures. 2019; 158:66–75.

